

## LONGITUDINAL SPIN STRUCTURE AT COMPASS

Y. BEDFER

on behalf of the COMPASS collaboration

CEA/IRFU, Saclay, France      *E-mail address:* Yann.Bedfer@cern.ch

Received 1 February 2011;      Accepted 14 December 2011

Online 13 February 2012

COMPASS is a fixed-target experiment at CERN's Super-Proton-Synchrotron. Part of its physics program is dedicated to the spin structure of the nucleon, which it studies with a 160 GeV polarized muon beam and polarized targets. An overview of its measurements performed with longitudinal target polarization is given. In particular, recent results, concerning the gluon polarization, the separation of the contributions of the individual quark flavors and the test of the Bjorken sum rule, are presented.

PACS numbers: 13.60.-r, 13.88.+e, 14.20.Dh

UDC 539.125, 539.171

Keywords: nucleon spin structure, longitudinal target polarization, polarized 160 GeV muon beam, gluon polarization, Bjorken sum rule

### 1. Introduction

COMPASS follows a series of experiments studying the spin structure of the nucleon via inclusive deep inelastic scattering (DIS). At leading twist, i.e. limiting oneself to terms scaling modulo logarithms, and after integrating over the parton transverse momentum,  $k_T$ , this spin structure is fully determined by two sets of parton distributions: the helicity difference,  $\Delta q(x, Q^2)$ , and transversity,  $\Delta_T q(x, Q^2)$ . Although inclusive DIS has provided many insights into the  $\Delta q$ , it suffers from several limitations: the gluon distribution does not couple directly, but instead must be inferred from the evolution of quark distributions; only electromagnetic currents can be used (neutrino scattering from polarized targets being impractical) and therefore quarks and anti-quarks enter symmetrically and cannot be disentangled;  $\Delta_T q$  distributions, which are chiral odd, decouple altogether. COMPASS attempts to overcome these limitations by resorting to semi-inclusive measurements, both in DIS and photoproduction regimes. In this way, it can access the transversity distributions, using a transversely polarized target, and access by the same token some of the unintegrated, transverse momentum dependent (TMD) distributions. For these, the reader is referred to the paper of Christian Schill [\*]. I will report on my side on the  $k_T$ -integrated helicity aspect of the programme (carried out exclu-

sively with a longitudinally polarized target), covering the inclusive measurements as well as the semi-inclusive ones. The COMPASS physics programme includes also hadron spectroscopy studies and  $\chi$ PT tests, performed with a hadron beam, *cf.* the paper by Alexander Austregesilo [†].

## 2. Spin crisis/spin problem

The main conclusion of the inclusive DIS experiments is that the quarks and anti-quarks carry little of the nucleon longitudinal spin. This result follows from equation (1):

$$\begin{aligned} \frac{1}{2} \int g_1^p(x) dx = & (\Delta\Sigma_u - \Delta\Sigma_d)/12 + (\Delta\Sigma_u + \Delta\Sigma_d - 2\Delta\Sigma_s)/36 + (\Delta\Sigma_u + \Delta\Sigma_d + \Delta\Sigma_s)/9 \\ & + \text{QCD corrections} + \mathcal{O}(1/Q^2) \end{aligned} \quad (1)$$

relating the first moment of the structure function  $g_1^p$  measured in inclusive DIS to the moments  $\Delta\Sigma_q = \Delta q + \Delta\bar{q}$  of the quark distributions, in which the non-singlet terms are scale invariant and can be related to matrix elements known from neutron and hyperon  $\beta$  decay, and the singlet term  $\Delta\Sigma = \Delta\Sigma_u + \Delta\Sigma_d + \Delta\Sigma_s$  is precisely the total spin of quarks and anti-quarks.

This experimental outcome contradicts the expectations of quark models of the nucleon. A statement that came to be known as the “spin crisis”. (It has to be noted though, that recent developments in the quark model calculations [1] claim to have closed the gap.)

One way out of the contradiction, put forward by several authors [2, 3, 4], relies on one of the QCD correction terms, *viz.* that arising from the U(1) axial anomaly  $-3\alpha_s/2\pi \Delta G$ , where  $G$  is the gluon distribution, which is anomalous in the sense that it does not vanish at infinite  $Q^2$ . It is therefore necessary to estimate  $\Delta G$  to determine whether it is large enough to account for the value of  $g_1$ .

$\Delta G$  is also interesting in its own right, for its direct contribution to the nucleon’s spin budget,

$$\frac{1}{2} = \frac{1}{2} \Delta\Sigma + \Delta G + L_z,$$

where  $L_z$  represents the orbital momentum of the partons.

## 3. Dedicated measurements of $\Delta G$ : Open charm vs. high $p_T$

The gluon distribution can be inferred from the evolution of quark distributions with  $Q^2$ . In the polarized case, however, DIS data cover too small a range in  $Q^2$  for this method to significantly constrain  $\Delta G$ . The fit of world polarized DIS data

by COMPASS [5] exemplifies this situation. Therefore, one can only access  $\Delta G$  via semi-inclusive channels.

In COMPASS, we explore two such channels: open charm production and high transverse momentum (high  $p_T$ ) hadron production. The two share a set of common features. Factorization theorems ensure that, in the presence of a large scale, the cross-section can be written as a convolution of partonic cross-sections, calculable perturbatively, and quark and gluon distributions. And for both channels, this scale can be set irrespective of  $Q^2$ , by the charm mass and the  $p_T$ , respectively. Both have also been successfully used to directly measure the unpolarized gluon distribution at the HERA collider experiments (with the difference that high  $p_T$  refers to the production of jets there) [6, 7]. But they represent diametrically opposed trade-offs between the conflicting requirements of statistics and purity. Open charm is the purest. It provides a model-independent access to  $\Delta G/G$  and for this reason remains our golden channel. It is presented first. Next, the high  $p_T$  case is presented, subdivided into several sub-cases depending upon the  $Q^2$  of the exchanged photon. For the start, some experimental essentials are described.

#### 4. *Experimental essentials*

The COMPASS spectrometer is described in details in Ref. [8]. I recall that it uses a beam of 160 GeV muons, with an intensity of  $2 \cdot 10^8$  *per* spill of  $\sim 15$  s and a polarization of  $76 \div 80\%$ , and polarized deuteron and proton targets, in 2002–2006 and in 2007, respectively. Otherwise, it comprises two stages, for low and high momenta respectively, equipped with tracking, calorimetry and particle identification (muon absorbers in both stages and RICH in only the first one).

Its experimental setup was designed to allow a precise determination of asymmetries. An important point in this respect is the control of fake asymmetries. We achieve it thanks to the simultaneous measurement of both parallel and anti-parallel spin states in two oppositely polarized target cells, upstream  $u$  and downstream  $d$ , and to a frequent reversal of target spin orientations, so that fluctuations in acceptance and incident muon flux cancel out in the formula for the counting asymmetry  $A$ ,

$$A = \frac{1}{2} \left( \frac{N_u^{\uparrow\uparrow} - N_d^{\uparrow\downarrow}}{N_u^{\uparrow\uparrow} + N_d^{\uparrow\downarrow}} + \frac{N_d^{\uparrow\uparrow} - N_u^{\uparrow\downarrow}}{N_d^{\uparrow\uparrow} + N_u^{\uparrow\downarrow}} \right), \quad (2)$$

where  $\uparrow\uparrow$  and  $\uparrow\downarrow$  denote the two spin states. (Note that weighted asymmetries are used instead of (2) in all calculations presented below.)

The reversal of target spins is most frequently performed by field rotation. This rotation induces a small change in the acceptances of the  $u$  and  $d$  cells, which is hence correlated with the configuration of spin states. In order to correct for this effect, a full re-polarization is performed periodically, allowing a spin reversal in constant field.

An even better control of the instrumental asymmetries is achieved starting with

the 2006 run, where the target is divided in 3 ( $1/4 \uparrow$ ,  $1/2 \downarrow$ ,  $1/4 \uparrow$  and *vice-versa*), so that both spin states have permanently the same average acceptance.

The cross-section helicity asymmetry,  $A_{\parallel}$ , is related to the counting asymmetry by factors describing the polarization of the incoming particles,  $P_{\mu}$  for the beam,  $P_T$  and  $f$  for the target polarization and for the, process dependent, dilution factor. It is best expressed as  $A_{\parallel}/D$ ,

$$A_{\parallel}/D = A / (P_{\mu} \times P_T f \times D),$$

where one takes also into account a kinematical factor,  $D$ , describing the polarization transfer from the muon to the photon.  $D$  is process dependent and typically averages to  $\sim 60\%$ . Typical values for the LiD polarized deuteron target are  $P_T \simeq 50\%$  and  $f \simeq 40\%$ , yielding a figure of  $\sim 10\%$  for the overall dilution factor relating the physics asymmetry of interest to the experimental asymmetry. For the polarized proton target ( $\text{NH}_3$ ), the corresponding numbers are  $P_T \simeq 90\%$  and  $f \simeq 14\%$ , and  $\sim 6\%$  overall factor.

During its first four years of running from 2002 to 2004 and in 2006, the experiment has accumulated  $\sim 2.5 \text{ fb}^{-1}$  of data with its deuteron target polarized longitudinally. In 2007, an additional  $\sim .5 \text{ fb}^{-1}$  was recorded with a longitudinally polarized proton target.

Electromagnetic calorimetry has been progressively installed in both spectrometer stages next to the already existing hadronic one. It is not yet included in the muon data analysis.

## 5. $\Delta G$ from open charm

This channel was discussed by many authors [9, 10] as a good candidate to access  $\Delta G$ . The gluon distribution enters at leading order via the photon-gluon fusion (PGF)  $\gamma^* g \rightarrow c\bar{c}$ , provided that there is no significant charm content in the nucleon within the relevant kinematical domain and hence direct charm excitation  $\gamma^* c \rightarrow c$  does not contribute. This requirement is excellently fulfilled at our low COMPASS scales, except for a possible intrinsic charm, enhanced in the valence region [11]. The latter would however yield open charm at high Bjorken  $x_B$  (not to be confused with the scaling variable  $x_g$  at which PGF probes the gluons), whereas our measured cross-section turns out to lie in the  $10^{-4} < x_B < 10^{-2}$  range. Charm production proceeding *via* resolved photons is also expected to be small in the forward rapidity domain covered by our fixed target setup [12].

In COMPASS we tag open charm, and hence PGF, by the production of a  $D^0$  meson. The  $D^0$  meson can easily be reconstructed from its decay into, *e.g.*,  $K$  and  $\pi$ , where the  $K$  is identified with the RICH. The main difficulty lies in the associated combinatorial background. This is a major concern in our experiment, where the vertex resolution is not sufficient to resolve the decay vertex from the primary vertex, because of the thickness of the target.

Special care is therefore taken to optimize the use of the data. First, the favorable cases when the  $D^0$  comes from a  $D^* \rightarrow D^0\pi$  decay are counted separately, *cf.* Fig. 1. Secondly, kinematical cuts are applied, on the fraction  $z_D$  of the energy of the virtual photon carried by the  $D$  meson, and on its decay angle measured in its rest frame, relative to its direction of flight. The signal over background ratios  $S/B$  achieved by these cuts are of the order of 1/10 and 1/1 for the  $D^0$  and  $D^*$  samples respectively. Thirdly, a weighting procedure is applied for the computation of the average asymmetry

$$\langle A \rangle = \frac{1}{P_T} \frac{\sum_i^{\uparrow\uparrow} w_i - \sum_i^{\uparrow\downarrow} w_i}{\sum_i^{\uparrow\uparrow} w_i^2 + \sum_i^{\uparrow\downarrow} w_i^2}, \quad w_i = f P_\mu a \langle S/(S+B) \rangle, \quad (3)$$

where  $S/(S+B)$  is the signal strength and  $a$  is an analyzing power related term. The weights are calculated for each event based on neural network (NN) parametrizations of these two quantities in terms kinematical variables.

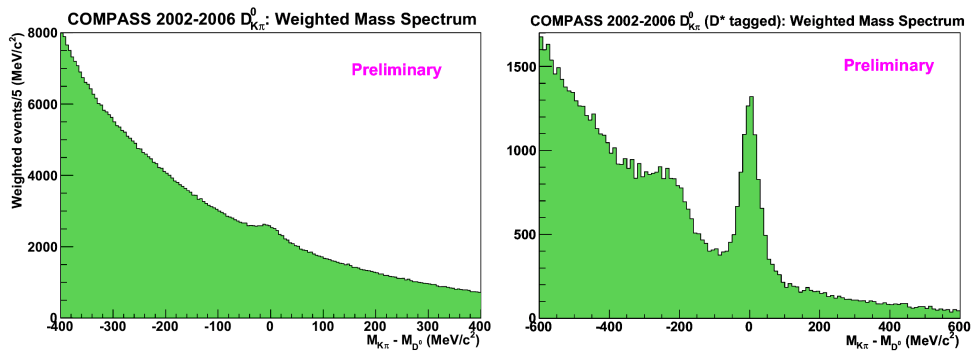


Fig. 1.  $D^0$  peak in the  $K\pi$  invariant mass distribution for all events (left) and  $D^*$ -tagged events (right) in [2002,2006] data. The mass distribution are weighted according to the scheme described in the text. The bump showing up at low mass in the  $D^*$  case arises from  $D^0 \rightarrow K\pi\pi^0$ , decays, where the  $\pi^0$  goes undetected. These are counted separately. So are  $D^*$ 's decaying into  $D^0\pi \rightarrow (K\pi^+\pi^-)\pi$ .

In order to derive the gluon polarization from the asymmetry, one need to go from the hadron level where the measurement is done to the parton level where the analyzing power of the hard processes can be calculated. In COMPASS, we consider two approaches for achieving this last step.

In the first approach, we restrict ourselves to LO ( $\mathcal{O}(\alpha\alpha_S)$ ), and carry the derivation to the end. We generate the parton level kinematics with a Monte Carlo simulation of the experiment based on the event generator AROMA [13], which computes the exact PGF matrix element with massive quarks to produce charmed hadrons, while turning off parton showers, so as to have a consistent LO description. We then calculate the analyzing power  $a_{LL}$  according to the LO polarized and unpolarized matrix elements given in Ref. [14] on a per event basis, and then parametrize it as a function of the hadron level kinematics using a NN, for each of

the hadronic final states of interest. It typically yields an  $\sim 80\%$  correlation with  $a_{LL}$  true value. This parameterization is entered, as  $a = a_{LL}$ , in Eq. (3), which then directly gives the average gluon polarization  $\langle \Delta G/G \rangle = \langle A \rangle$ . A preliminary analysis of the full statistics recorded in 2002–2007 yields

$$\langle \Delta G/G \rangle = -0.08 \pm 0.11(stat.) \pm 0.03(syst.) \quad \text{at } x_g = 0.11_{-0.05}^{+0.11} \quad \text{and } \mu^2 = 13 \text{ GeV}^2,$$

where the systematics are dominated by the instrumental asymmetry, which is evaluated on a higher statistics sample, and  $x_g$  and  $\mu^2$  are extracted from the MC simulation.

In the second approach, we only release the hadron level asymmetry, and leave the task of extracting  $\Delta G/G$  to an independent analysis. In that case, we choose to enter a depolarizing factor  $D$  in the event weight of Eq. (3). When doing this, we have to care about a possible correlation between the quantity that will have to be averaged over in the extraction of  $\Delta G/G$ , *viz.*  $a_{LL}/D$ , and variables included in the weight. In order to minimize any bias, the asymmetry is evaluated independently in several  $p_T \times E$  bins, where  $p_T$  and  $E$  are the transverse momentum and energy of the produced  $D^0$  meson. An example of an NLO extraction of  $\Delta G/G$  from such a set of asymmetry bins is given in Ref. [15].

### 5.1. $\Delta G$ from high $p_T$

The alternative channel used to access  $\Delta G/G$  consists in requiring hadron production at a high transverse momentum,  $p_T$ , with respect to the virtual photon [16]. This suppresses  $\gamma^* q \rightarrow q$  events, where the fragmenting quark goes into the direction of the photon. The suppression is not perfect, however, and the cross-sections receive also contributions from competing partonic channels, involving either direct or resolved photons. They correspond to the leading order processes depicted in Fig. 2, where the processes sensitive to the gluon distribution in the nucleon are shown first. In order to gain information about the gluon distribution from this bundle of processes, we have considered two different approaches. They most significantly differ in the way they fold the partonic level QCD calculations with the soft fragmentation process and the instrumental acceptance. I will refer to them in what follows as the Monte Carlo based and the NLO collinear pQCD analyses.

### 5.2. Monte Carlo based high $p_T$ analyses

The Monte Carlo method relies on the following approximation for the LO expansion of the cross-section helicity asymmetry

$$A_{\parallel} \simeq (R_{\text{PGF}} \langle a_{LL}^{\text{PGF}} \rangle + \sum R_i \langle D a_{LL}^i \Delta f/f \rangle) \Delta G/G + A_{\text{Background}}$$

where the summation runs over all resolved photon processes sensitive to the gluon distribution, the  $R$  factors represent the fraction of events for a given process,  $a_{LL}$  is its analyzing power,  $\Delta f/f$  are the polarizations of the partons in the resolved

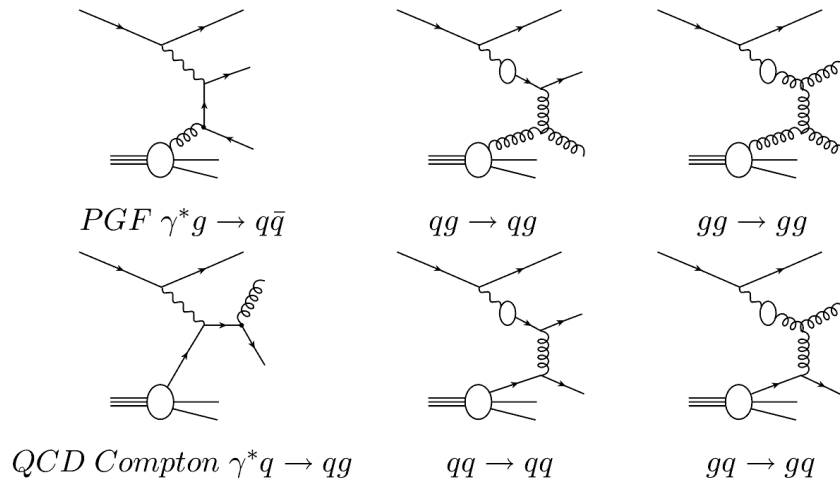


Fig. 2. High  $p_T$  hadron production processes in LO pQCD.

photon and  $A_{\text{Background}}$  is the contribution to the asymmetry of all remaining processes. In order to retrieve  $\Delta G/G$ , the  $R$  fractions,  $A_{\text{Background}}$  and the parton level kinematics defining  $a_{LL}$  need be determined by a simulation of the experiment. In COMPASS, we consider independently two different kinematical regimes, the DIS regime at  $Q^2 > 1 \text{ GeV}^2$  and the photoproduction regime at  $Q^2 < 1 \text{ GeV}^2$ . And for the simulation, we resort to the Monte Carlo event generators, LEPTO [17] and PYTHIA [18], respectively. The two cases share a number of common features. As was already mentioned, they both rely on a LO approximation. And for both, the event selection follows a same path. In particular, the production of a pair of high  $p_T$  hadrons is required. But the two cases are attractive in their own right. The photoproduction case yields much higher statistics, a factor 10. But the DIS event generation is theoretically better grounded:  $Q^2$  provides the hard scale and eliminates the need for modeling events from soft processes that pass the  $p_T$  selection cut through fragmentation. The  $Q^2$  allows also to neglect the resolved photons and the dependence upon the poorly known polarized structure of the photon they introduce.

The Monte Carlo method does not require any modeling of the gluon polarization  $\Delta G(x)$  as a function of  $x$  and makes a direct measurement of the average value of  $\Delta G/G$  over a given  $x_g$  range. It has been so far COMPASS's favored approach.

### 5.2.1. High $p_T$ , $Q^2 < 1 \text{ GeV}^2$

This channel was the subject of a publication, Ref. [19]. An analysis of a larger data set, 2002–2004, has since been released, yielding

$$\langle \Delta G/G \rangle = 0.016 \pm 0.058(\text{stat.}) \pm 0.054(\text{syst.}) \text{ at} \\ x_g = 0.085_{-0.035}^{+0.071} \text{ and } \mu^2 = 3 \text{ GeV}^2.$$

where the main contribution to the systematics is that from MC, which is evaluated by exploring the parameter space of the generator. The polarized structure of the photon is taken into account by considering two extreme scenarios, minimally and maximally polarized, as explained in Ref. [20]. The associated systematics remains small, due the dominance of the perturbatively calculable point-like structure in our kinematical domain.

### 5.2.2. High $p_T$ , $Q^2 > 1 \text{ GeV}^2$

In this case, we take advantage of the fact that the hard scale can be provided by the photon virtuality  $Q^2$ , to analyze simultaneously high  $p_T$  and inclusive data samples. We expand the asymmetry of these two samples ( $S$ ) in term of  $R$  factors and analyzing power  $a_{LL}$  according to the following approximation,

$$A_{\parallel}^S(x) \approx \frac{\Delta G}{G}(x_g) \langle a_{LL}^{\text{PGF}} \rangle \mathcal{R}_{\text{PGF}}^S + A_1(x_C) \langle a_{LL}^C \rangle \mathcal{R}_C^S + A_1(x) D \mathcal{R}_L^S \quad (4)$$

where we consider three processes, *viz.* PGF, QCD Compton ( $C$ ) and photo-absorption, and neglect resolved photons (based on simulations done with the MC generator RAPGAP [21]). This allows the most direct access to  $\Delta G$ , without any reliance on model assumptions for the functional shapes of the polarized parton distributions. All parameters appearing in the set of two equations built on Eq. (4), and needed to extract  $\Delta G$ , are obtained from Monte Carlo simulations. It is therefore crucial to ensure that they accurately reproduce the data. To do so, we have had to tune the fragmentation and intrinsic  $k_T$  in LEPTO. An example of the quality of the agreement achieved is given in Fig. 3. The simulations are then parametrized in terms of hadron level kinematics using neural networks.

The analysis of our 2002–2006 deuteron data yields the following result

$$\begin{aligned} \langle \Delta G/G \rangle &= 0.125 \pm 0.060(\text{stat.}) \pm 0.065(\text{syst.}) \text{ at} \\ x_g &= 0.09_{-0.04}^{+0.08} \text{ and } \mu^2 = 3.4 \text{ GeV}^2. \end{aligned}$$

where the main contributions to the systematics come from the MC and the approximations made in the expansion of the asymmetries with Eq. (4). For the evaluation of the MC contribution, several settings of the LEPTO generator were varied, including the cut-off scheme used to regularize the partonic cross-sections. The analysis was also done independently on three sub-samples, defining three, overlapping,  $x_g$  bins. No trend in  $\Delta G/G$  *vs.*  $x_g$  could be evidenced.

### 5.3. NLO collinear pQCD analysis of high $p_T$ photoproduction

In this approach to the high  $p_T$  analysis, the soft hadronization is modeled by independent fragmentation and the finite acceptance of the spectrometer is taken into account by applying acceptance cuts directly to the parton level kinematics, while Monte Carlo is only used to correct for the inefficiency and the finer details of the acceptance of the instrumental setup. This allows to extends the pQCD



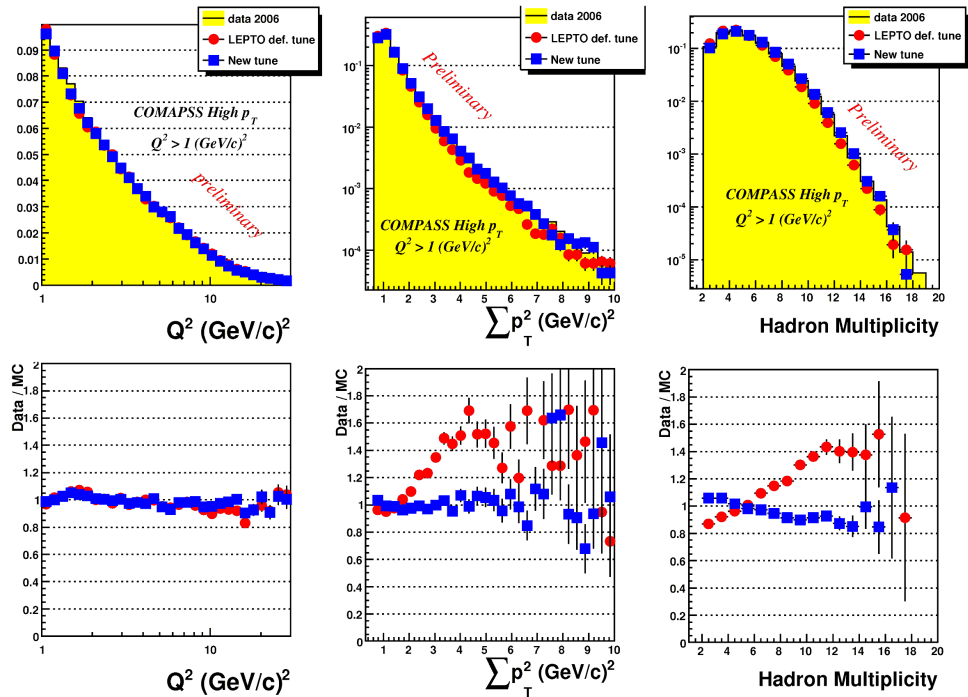


Fig. 3. Data vs. MC for some kinematical distributions of the high  $p_T$ ,  $Q^2 > 1 \text{ GeV}^2$  events, illustrating the agreement obtained with COMPASS tuning (see text). The upper plots show MC points superimposed on histograms of the data. The lower plots show the data/MC ratios.

calculation to NLO ( $\mathcal{O}(\alpha_s^2)$ ). The calculations for the COMPASS case have been done, at NLO, for two sub-cases: single hadron production [22] and hadron pair production [23]. In these calculations, a parametrization of  $\Delta G(x)$  vs.  $x$  is assumed and the differential asymmetry is determined as a function of  $p_T$ .  $\Delta G/G$  can then be constrained by adjusting the parametrization for the calculated asymmetry to fit the data. This will be eventually done in a global fit, adjusting both quark and gluon spin densities.

The analysis of the COMPASS data along these lines is under way. A first and mandatory step is to check that the unpolarized  $p_T$  distribution is correctly described by the theoretical calculation.

## 6. $\Delta G$ summary

The COMPASS preliminary results discussed *supra* are plotted on Fig. 4. They constrain the gluon distribution in a restricted  $x$  domain. In order to constrain the first moment  $\Delta G$ , we compare them with the various scenarios put forward to fit world DIS data. They then clearly favor low values of  $\Delta G$ , at a scale of  $3 \text{ GeV}^2$ ,

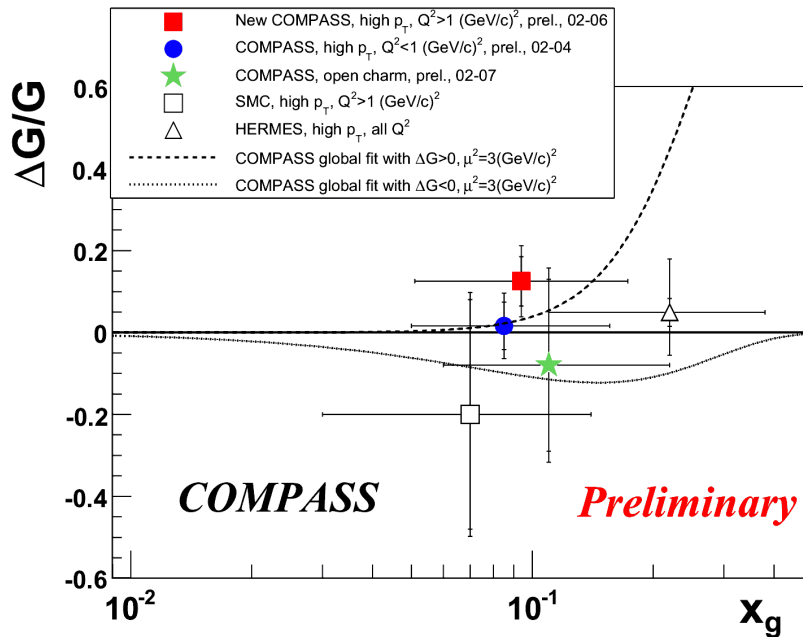


Fig. 4. Summary of the direct measurements of  $\Delta G/G$ . The three COMPASS results are plotted, together with those of HERMES [24] and SMC. The two error bars correspond to the statistical uncertainty alone, and to its quadratic sum with the systematic error. The horizontal bar represents the  $x$ -range of the measurement. The curves show  $\Delta G/G(x)$  at  $Q^2 = 3 \text{ GeV}^2$  for the two solutions of COMPASS NLO QCD fit, cf. text in section 7, with the unpolarized  $G(x)$  taken from MRST2004 [25].

and dismiss as very unlikely the axial anomaly scenario whereby a  $\Delta G$  of the order of  $2 \div 3$  would account for the small value of the first moment of  $g_1$ .

However, these results remain consistent with a range of possible shapes, as exemplified by their compatibility with our two COMPASS solutions, cf. Fig. 4. In order to go further, one needs to carry out a global NLO QCD fit, as is done by DSSV [30], who combine polarized DIS data and  $\vec{p}\vec{p}$  data from RHIC. Our open charm asymmetries and photoproduction high- $p_T$  data could be included in such a fit.

## 7. Inclusive measurements

Simultaneously with the acquisition of  $\Delta G$  dedicated data, the inclusive double spin asymmetry  $A_{\parallel}$  was measured, both on the deuteron ( $d$ ), 2002–2006, and on the proton ( $p$ ), 2007. In the COMPASS kinematical domain, the approximation

$$g_1 \simeq \frac{A_{\parallel}}{D} F_1 \quad (5)$$

holds to very good precision and the sole measurement of  $A_{\parallel}$  suffices to determine  $g_1$ . The proton and deuteron results were the subject of two independent publications [5, 26]. In both cases, they improve the precision of the world data at small  $x$ , extending their range down to  $x = 0.004$ . The improvement is particularly significant in the  $d$  case, where in addition, the new COMPASS data happen not to support the decrease of  $g_1^d$  as  $x \rightarrow 0$  predicted by earlier QCD fits of world data. This has two consequences. It first brings about an increase in the evaluations of the total quark spin  $\Delta\Sigma$  [5, 27]. Secondly, since the behavior of  $g_1$  at low  $x$  is driven by the gluons at higher  $x$  [28], it opens up the possibility of a negative or sign changing  $\Delta G(x)$  at COMPASS  $Q^2$ 's. The COMPASS fit [5] finds the two solutions  $\Delta G < 0$  and  $\Delta G > 0$  to be equally probable.

The combination  $g_1^{p-n}$ , that one derives from  $g_1^p$  and  $g_1^d$ , is of special interest, since its  $Q^2$  evolution decouples from the singlet and gluon spin densities, yielding, up to higher twist terms, the Bjorken sum rule

$$\int g_1^{p-n}(x)dx(Q^2) = 1/6 g_A/g_V C^{NS}(Q^2) \tag{6}$$

where  $C^{NS}$  is the non-singlet Wilson coefficient, given as a perturbative series in  $\alpha_S$ , and the ratio  $g_A/g_V$  is known from neutron  $\beta$  decay. The determination of the LHS of Eq. 6 involves an extrapolation to  $x = 0$ , which we achieve *via* a NLO QCD fit of our  $g_1^{p-n}(x)$  data, *cf.* Fig. 5. The test of the Bjorken sum rule can be viewed as a validation of the small- $x$  behavior assumed for  $g_1$ , or as a constraint put on the models used for evaluating higher twist terms. Performing it on the sole COMPASS data allows to get rid of part of the systematics. We find

$$|g_A/g_V| = 1.28 \pm 0.07(stat.) \pm 0.10(syst.)$$

with a precision still limited by the systematics, mainly due to the uncertainty on the beam polarization.

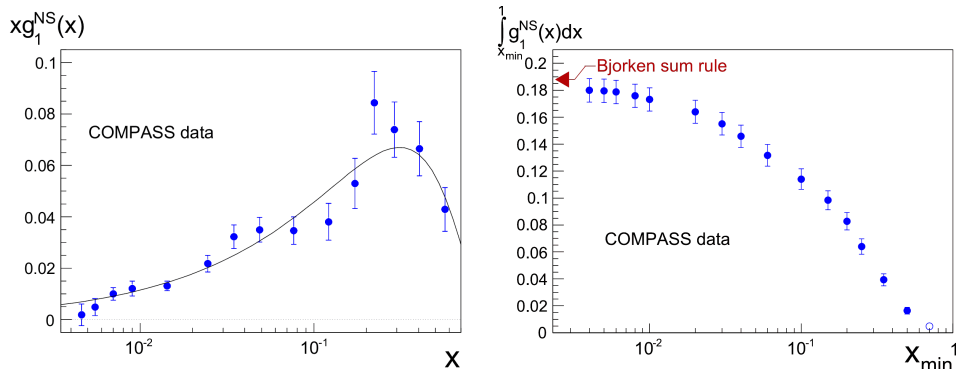


Fig. 5. Left: NLO QCD fit of COMPASS  $g_1^{p-n}(x)$  data (shown at a  $Q^2$  of  $3 \text{ GeV}^2$ ). The errors are statistical only. Right:  $\int_{X_{min}}^1 g_1^{p-n} dx$  as a function of  $X_{min}$ .

## 8. *Semi-inclusive measurements*

Semi-inclusive measurements, SIDIS, where in addition to the scattered lepton, a hadron is also detected, allow to disentangle quarks and anti-quarks. Of particular interest along this line is a possible flavor symmetry breaking in the light sea,  $\Delta\bar{u} \neq \Delta\bar{d}$ , given the well established difference between  $\bar{u}$  and  $\bar{d}$  in the unpolarized case.

SIDIS also provides an independent access to the polarized strangeness distribution. Inclusive data yield a determination of its first moment  $\Delta s + \bar{s}$  via Eq. (1) and the SU(3) scheme of the measured baryon octet  $\beta$ -decays, which turns out to be negative. But they only poorly constrain its shape as a function of  $x$ . Global QCD fits of world DIS data have long assumed it to be uniformly negative. The result of an analysis by the HERMES collaboration of charged kaon production came to contradict this assumption [29].

The most promising way to handle the SIDIS data, and to address the seeming contradictions they lead to, is a global NLO QCD fit of both inclusive DIS and SIDIS asymmetries. Several groups have undertaken the task [30–32].

In COMPASS, we have measured the longitudinal virtual photon asymmetries  $A_1^{h,N}$  for hadron  $h = \pi^\pm, K^\pm$  and target  $N = p, d$  [33, 34]. We extract the required hadron production data from our inclusive DIS samples, by identifying the hadron with the RICH. And we determine  $A_1$  from the double spin asymmetry  $A_{||}$  using the same approximation as employed in the inclusive case, cf. Eq. (5).

The ultimate use of these data is to improve the accuracy of global fits. Our  $A_1^{h,d}$  results have already been included in Ref. [32]. We nevertheless think that analyses limited to our sole COMPASS data, performed at LO order, are still relevant. They allow to keep systematics under control. And they can pinpoint specific areas of concern. As an example, the result of our combined analysis of all COMPASS data is shown in Fig. 6. It reproduces the features observed by the global fits concerning the flavor symmetry breaking of the light sea and the strangeness distribution. But it allowed us to evidence the strong sensitivity of the flavor separation upon the values of the fragmentation functions, in particular upon the ratio of the  $\bar{s}$ -quark to  $u$ -quark fragmentations to  $K^+$ .

## 9. *Outlook*

The COMPASS programme of inclusive and semi-inclusive measurements of polarized muon-nucleon scattering has already produced many interesting results concerning the longitudinal spin structure of the nucleon. We plan to complete it by taking more data on polarized protons in 2012, bringing them to the level of precision already obtained on polarized deuterons. The main goal is to contribute to the solution of the strangeness conundrum.

On the analysis side, our aim is to get our data included in global NLO QCD fits. We intend to carry on with the study of high  $p_T$  hadron photoproduction outlined in section 5.3. And we plan to contribute to a better understanding of the

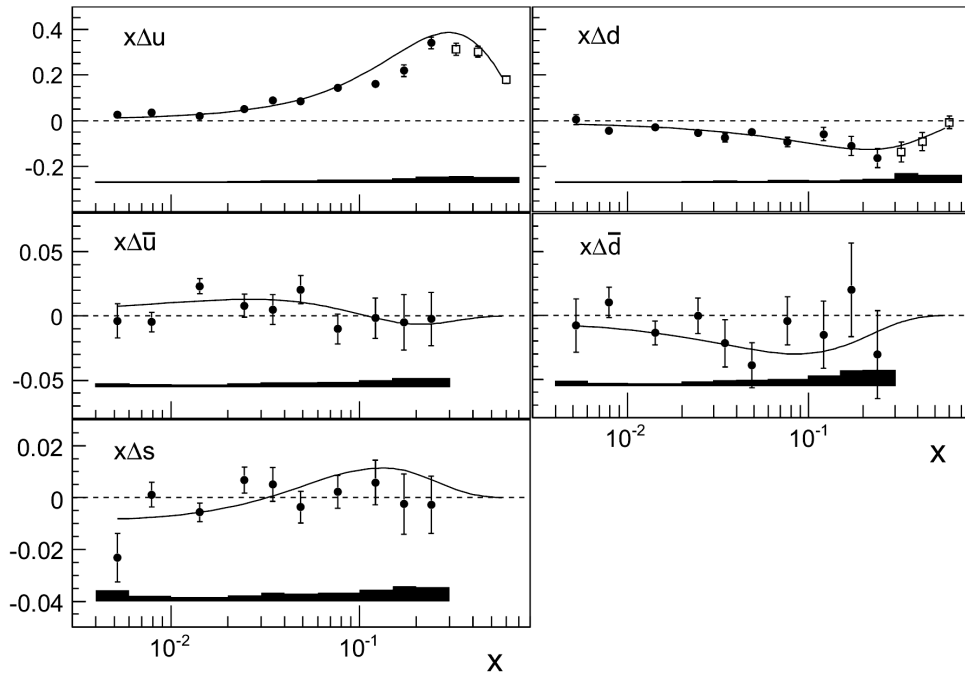


Fig. 6. The quark helicity distributions  $x\Delta q$ ;  $q = u, d, \bar{u}, \bar{d}, s+\bar{s}$  at  $Q^2 = 3 \text{ GeV}^2$  as a function of  $x$ . The values for  $x < 0.3$  (black dots) are derived from a LO analysis of SIDIS asymmetries using DSS [35] fragmentation functions. Those at  $x > 0.3$  (open squares) are derived from inclusive DIS assuming  $\Sigma\Delta\bar{q} = 0$ . The bands show the systematic errors. The curves show the NLO predictions of the DSSV fit [30].

fragmentation process in the COMPASS kinematical range by providing unpolarized multiplicity data, that could be included in a global analysis of fragmentation functions such as DSS [35].

For the long term, the COMPASS collaboration has submitted a proposal to the SPS Steering Committee [36], focusing on GPD and Drell-Yan measurements, *cf.* the presentation of Nicole d'Hose at Conference NAPP-2010 [†].

#### References

- [\*] Ch. Schill, *Fizika B* **20** (2011) 93 (this volume).
- [†] A. Austregesilo, *Fizika B* **20** (2011) 117 (this volume).
- [1] F. Myhrer and A. W. Thomas, *Phys. Lett. B* **663** (2008) 302; [arXiv:0709.4067 [hep-ph]].
- [2] A. V. Efremov and O. V. Teryaev, JINR-E2-88-287.

- [3] G. Altarelli and G. G. Ross, Phys. Lett. B **212** (1988) 391.
- [4] R. D. Carlitz, J. C. Collins and A. H. Mueller, Phys. Lett. B **214** (1988) 229.
- [5] V. Y. Alexakhin et al. [COMPASS Collaboration], Phys. Lett. B **647** (2007) 8; [arXiv:hep-ex/0609038].
- [6] B. W. Harris, arXiv:hep-ph/9909310.
- [7] A. M. Cooper-Sarkar, arXiv:hep-ex/0511058.
- [8] P. Abbon et al. [COMPASS Collaboration], Nucl. Instrum. Meth. A **577** (2007) 455; [arXiv:hep-ex/0703049].
- [9] A. D. Watson, Z. Phys. C **12** (1982) 123.
- [10] M. Glück and E. Reya, Z. Phys. C **39** (1988) 569.
- [11] A. D. Martin, W. J. Stirling, R. S. Thorne and G. Watt, Eur. Phys. J. C **63** (2009) 189; [arXiv:0901.0002 [hep-ph]].
- [12] M. Stratmann and W. Vogelsang, arXiv:hep-ph/9708243.
- [13] G. Ingelman, J. Rathsman and G. A. Schuler, Comput. Phys. Commun. **101** (1997) 135; [arXiv:hep-ph/9605285].
- [14] I. Bojak and M. Stratmann, Nucl. Phys. B **540** (1999) 345; [arXiv:hep-ph/9807405].
- [15] K. Kurek, PoS D **IS2010** (2010) 160.
- [16] A. Bravar, D. von Harrach and A. Kotzinian, Phys. Lett. B **421** (1998) 349; [arXiv:hep-ph/9710266].
- [17] G. Ingelman, A. Edin and J. Rathsman, Comput. Phys. Commun. **101** (1997) 108; [arXiv:hep-ph/9605286].
- [18] T. Sjöstrand, L. Lönnblad, S. Mrenna and P. Skands, arXiv:hep-ph/0308153.
- [19] E. S. Ageev et al. [COMPASS Collaboration], Phys. Lett. B **633** (2006) 25; [arXiv:hep-ex/0511028].
- [20] M. Glück, E. Reya and C. Sieg, Eur. Phys. J. C **20** (2001) 271; [arXiv:hep-ph/0103137].
- [21] H. Jung, Comput. Phys. Commun. **86** (1995) 147.
- [22] B. Jäger, M. Stratmann and W. Vogelsang, Eur. Phys. J. C **44** (2005) 533; [arXiv:hep-ph/0505157].
- [23] C. Hendlmeier, M. Stratmann and A. Schäfer, arXiv:0706.3766 [hep-ph].
- [24] A. Airapetian et al. [HERMES Collaboration], [arXiv:1002.3921 [hep-ex]].
- [25] A. D. Martin, R. G. Roberts, W. J. Stirling et al., Phys. Lett. B **604** (2004) 61; [hep-ph/0410230].
- [26] M. Alekseev et al. [COMPASS Collaboration], Phys. Lett. B **690** (2010) 466; [arXiv:1001.4654 [hep-ex]].
- [27] E. Leader, A. V. Sidorov and D. B. Stamenov, Phys. Rev. D **75** (2007) 074027; [hep-ph/0612360].
- [28] R. D. Ball, G. Ridolfi, G. Altarelli et al., *What can we learn from polarized structure function data*

- [29] A. Airapetian et al. [HERMES Collaboration], Phys. Lett. B **666** (2008) 446; [arXiv:0803.2993 [hep-ex]].
- [30] D. de Florian, R. Sassot, M. Stratmann and W. Vogelsang, Phys. Rev. Lett. **101** (2008) 072001; [arXiv:0804.0422 [hep-ph]].
- [31] D. de Florian, G. A. Navarro and R. Sassot, Phys. Rev. D **71** (2005) 094018; [hep-ph/0504155].
- [32] E. Leader, A. V. Sidorov and D. B. Stamenov, Phys. Rev. D **82** (2010) 114018; [arXiv:1010.0574 [hep-ph]].
- [33] M. Alekseev et al. [COMPASS Collaboration], Phys. Lett. B **680** (2009) 217; [arXiv:0905.2828 [hep-ex]].
- [34] M. G. Alekseev et al. [COMPASS Collaboration], Phys. Lett. B **693** (2010) 227; [arXiv:1007.4061 [hep-ex]].
- [35] D. de Florian, R. Sassot and M. Stratmann, Phys. Rev. D **75** (2007) 114010; [hep-ph/0703242 [HEP-PH]].
- [36] The COMPASS collaboration, CERN-SPSC-2010-014, SPSC-P-340 (2010).
- [<sup>†</sup>] Nicole d'Hose, talk at 3<sup>rd</sup> Int. Conf. Nucl. Part. Phys. (NAPP-2010), Dubrovnik 3–8 October 2010, unpublished.

UZDUŽNA SPINSKA STRUKTURA PRI COMPASSU

COMPASS su mjerenja na mirnoj meti pri super protonskom sinkrotronu u CERNu. Dio programa njegovih istraživanja posvećen je spinskoj strukturi nukleona što se proučava sa snopom polariziranih muona energije 160 GeV i polariziranim metama. Izlaže se pregled mjerenja izvedenih s uzdužno polariziranim metama. Posebice se izlažu nedavni ishodi za gluonsku polarizaciju, razdjela doprinosa pojedinačnih kvarkovskih okusa i provjera Bjorkenovog pravila suma.